Colloidal lithography and Metal-Organic Chemical Vapor Deposition process integration to fabricate ZnO nanohole arrays

Maria Elena Fragalà [a,*], Cristina Satriano [a], Yana Aleeva [b], Graziella Malandrino [a]

[a] Dipartimento di Scienze Chimiche Università di Catania and INSTM UdR Catania, Viale Andrea Doria,6, Catania, Italy
[b] Scuola Superiore Università di Catania, Dipartimento di Scienze Chimiche Viale Andrea Doria, 6, Catania, Italy

ARTICLE INFO

ABSTRACT

A complete set up of optimal process conditions for an effective colloidal lithography/catalyst assisted MOCVD process integration is presented. It mainly focuses on the determination of the deposition temperature threshold for ZnO Metal-Organic Chemical Vapour Deposition (MOCVD) as well as the concentration of metal-organic silver (Ag) catalyst. Indeed, the optimization of such process parameters allows to tailor the ZnO film morphology in order to make the colloidal lithography/catalyst assisted MOCVD approach a valuable bottom up method to fabricate bi-dimensional ordered ZnO nanohole arrays.

© 2010 Elsevier B.V. All rights reserved.

1. Introduction

ZnO is a multifunctional material having intriguing semiconducting, optical, ferroelectric, piezoelectric, chemical and biochemical properties for a wide range of novel applications [1,2]. In particular ZnO nanowires and nanorods represent spatially controlled, highly functional nanostructures having remarkable physical and chemical properties [3–6].

ZnO nanowires can be produced using different metal catalysts and the metal selection is crucial to achieve the desired nanowire morphology and to avoid any potential detrimental contamination [7]. A catalyst particle deposited on a substrate acts as a preferential site for vapour absorption of the desired source material. As the source material is absorbed into the catalyst and the catalyst particle becomes supersaturated, the excess source material precipitates out and a 1D nanostructure grows [8]. Different catalysts can be used [9–11], Au being the most used for ZnO nanowire growth [12,13]. In fact, the use of Ag as an alternative catalyst has the drawback of temperature limitation (up to 500 °C) related to fast Ag oxidation which results in low-quality nanowires [8]. For this reason Ag has been much less explored as a catalyst for the growth of ZnO nanostructures.

On the other hand, the surface nanostructuring of metal oxide films in two-dimensional (2D) porous substrates is an intriguing strategy for various applications including microelectronics, sensing, catalysis, optics and biomedical science [14,15].

In this context, nanosphere lithography is emerging as an effective bottom up and flexible approach where self-assembled 2D colloidal nanoparticles [16] act as template or mask for producing 2D regular and nearly homogenous arrays of the desired materials [17]. Recently we reported on the fabrication of two-dimensional periodic ZnO arrays by a hybrid approach of colloidal lithography and MOCVD, based on silver catalyst-controlled ZnO growth [18].

In this paper we focus on optimization of experimental set up with a particular effort dedicated to study the MOCVD temperature deposition threshold and the relationship between initial concentrations of silver catalyst metal-organic precursor and ZnO deposition process parameters (deposition temperature and time), in order to tailor the morphology of ZnO films.

X-ray photoelectron spectroscopy and atomic force microscopy analyses are used as valuable methods to define the ZnO deposition temperature threshold, in terms of both thickness uniformity and film composition. Moreover, the scanning electron microscopy analyses integrate this study by evidencing the relationship between the silver catalyst concentration and the ZnO morphological control. The obtained results allow to set up the optimal experimental conditions for an effective colloidal lithography/catalyst assisted MOCVD process integration, in order to fabricate bi-dimensional ordered ZnO nanohole arrays.

2. Experimental

ZnO depositions on unpatterned or patterned (*via* colloidal lithography) silicon substrates have been performed in a hot wall tubular reactor, using a diamine (N,N,N′,N′-tetramethylethylenediamine) adduct of zinc bis-2 thenoyl-trifluoroacetonate [Zn(tta)$_2$·tmeda] [22]. Deposition conditions have been optimized through evaluation of

* Corresponding author. Dipartimento di Scienze Chimiche, Università di Catania. Viale Andrea Doria, 6, 95127 Catania, Italy. Tel.: +39 095 7385055; fax: +39 095 580138.
E-mail address: me.fragala@unict.it (M.E. Fragalà).
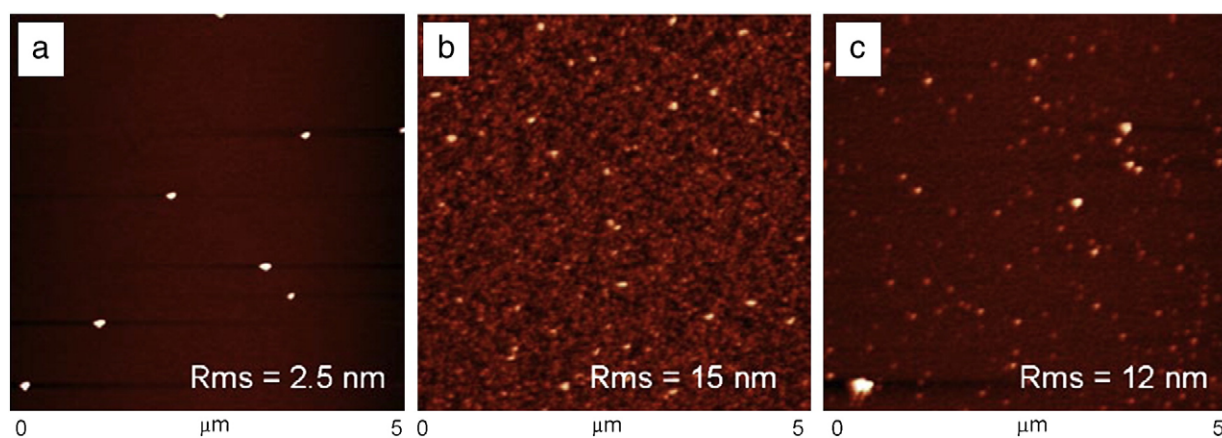
Fig. 1. AFM images of bare silicon substrate, before (a) and after ZnO thin film depositions at 300 °C, 40 min (b) and 400 °C, 5 min (c).

different growth temperatures, (ranging from 250° to 600 °C) and times (ranging from 5 min to 1 h).

Ag(hfa)·tetraglyme (Hhfa 1,1,1,5,5,5-hexafluoro-2,4-pentanedione; tetraglyme 2,5,8,11,14-pentaoxatetradecane) precursor, whose synthesis has been reported elsewhere [19,20], has been dissolved in Tetrahydrofuran (THF). The obtained solutions, having 0.1 M and 0.01 M concentrations, have been drop casted either on unpatterned or patterned silicon substrates, previously dipped in HF (7:1 HF/H_2O dilution, 1 min dipping time). Patterned silicon substrates have been obtained by dewetting driven self-assembly of polystyrene (PS) nanoparticles into close packed hexagonal arrays [21].

ZnO has been deposited by MOCVD either on silicon and unpatterned (Ag(hfa)tetraglyme initial concentrations of 0.1 M and 0.01 M) or patterned (Ag(hfa)tetraglyme initial concentration of 0.1 M) catalyst layers. Ar (150 sccm) and O_2 (150 sccm) have been used as carrier and reactive gas respectively.

The X-ray photoelectron experiments (XPS) have been carried out with a base pressure of 2×10^{-10} Torr using a PHI ESCA/SAM 5600 Multy technique spectrometer. A monochromatic Al K$_\alpha$ radiation source (h$\nu = 1486.6$ eV) has been used. The surface analysis of ZnO films has been conducted by acquiring both survey and narrow region scans at pass energies respectively of 187 eV and 11 eV, with an incremental step size of 1 eV for survey scans and 0.05 eV for the narrow scans, and a 0.8 mm slit width. Spectra have been acquired at a takeoff angle of 45° with respect to the samples surface. The samples have been sufficiently conductives that it has been not necessary to

supply electrons for charge compensation. The XPS signals have been analysed by using a peak synthesis program in which a nonlinear background is assumed and the fitting peaks of the experimental curve have been defined by a combination of gaussian (80%) and lorentzian (20%) distributions. The atomic compositions have been evaluated using sensitivity factors as provided by F V5.4A software.

Film surface morphologies have been investigated using a LEO Supra 55VP field emission gun scanning electron microscope (FEG-SEM).

Atomic force microscopy (AFM) images have been obtained in high amplitude tapping mode in air with an NT-MTD instrument. Golden silicon probes (NT-MTD) with a nominal resonant frequency of 190–325 kHz have been employed.

3. Results and discussion

In order to identify the deposition temperature threshold, ZnO thin films have been deposited at low temperatures (below 450 °C) on unpatterned silicon substrates. The AFM images (Fig. 1a–b) show the film morphology of ZnO films grown respectively at 300 °C (for 40 min, Fig. 1b) and 400 °C (for 5 min, Fig. 1c) in comparison with a bare silicon substrate (Fig. 1a). For both deposition conditions, it is evident that, notwithstanding the low temperatures used, the ZnO thin films are successfully grown on the substrates. The morphology of 300 °C, 40 m (Fig. 1b) deposited films clearly presents spherical grains, having dimensions of about 50 nm. The related overall surface roughness (Rq) is peaked at ~15 nm. The film deposited at 400 °C, 5 min (Fig. 1b) is characterised by a smoother surface (~12 nm). Therefore, we deduce that the latter film can be likely constituted by a continuous layer, with isolated large grains, as better visible in the related SEM image (Fig. 2). It is worthy to note that the AFM analysis (not shown) of ZnO deposited on silicon substrates at 250 °C, reveals the presence of isolated ZnO islands and confirms a limited deposition.

The AFM analysis is supported by XPS results, showing the typical Zn 2p$_{3/2}$ peak centered at 1022 ± 0.2 eV, that validates the presence of the ZnO layers onto silicon substrates. The average atomic compositions from XPS analysis are reported in Table 1.

It is worthy to note that the Zn content detected on the ZnO film deposited at 400 °C (~26%) is higher than that of the films deposited at 300 °C (~14%). However, while the latter film seems
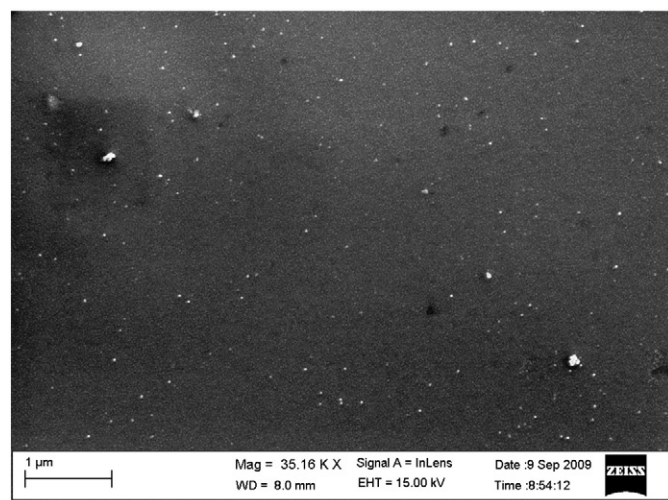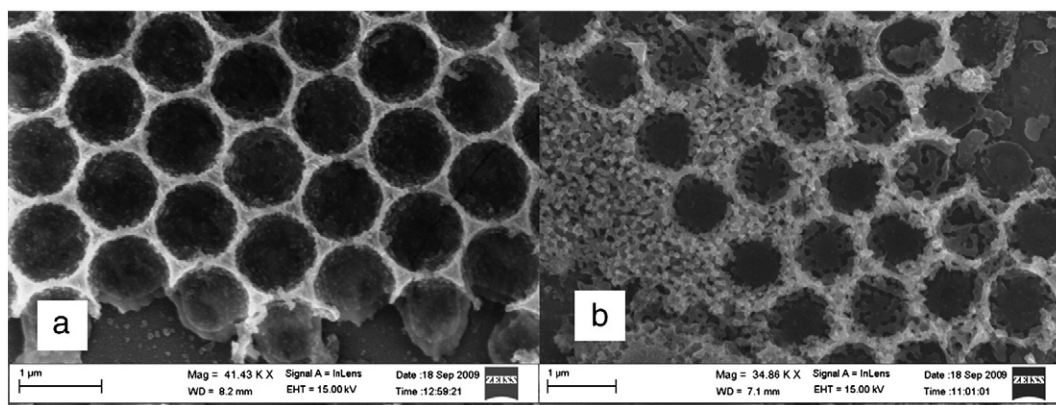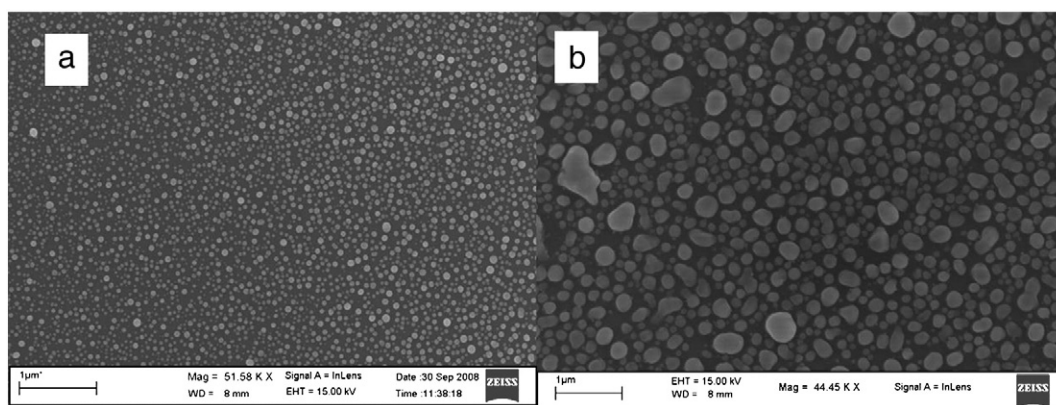

Fig. 2. SEM image (scale bar = 1 micron) of ZnO film deposited on Si at 400 °C, 5 min.

Table 1
XPS average atomic composition of ZnO films vs deposition temperature.

	Zn	C	O	Si
250 °C	1.6	21.7	39.4	37.3
300 °C	14.0	52.9	33.0	NA
400 °C	25.7	23.1	48.8	7.5

Fig. 3. SEM images (scale bar = 1 micron) of ZnO film deposited on Si substrates patterned with PS nanosphere: (a) 300 °C, 40 min, (b) and 400 °C, 5 min.


Fig. 4. SEM images (scale bar = 1 micron) of annealed silver film deposited on Si by spin coating (a) and drop casting (b).

to completely cover the substrate (silicon signal is not detected), on the ZnO film grown at 400 °C a silicon content of about 7% indicates the formation of ZnO islands. These findings confirm the morphological results of AFM and SEM analyses, i.e., the formation, working at 400 °C (5 min), of isolated large grains on a continuous film thinner than that deposited at 300 °C (40 min). Moreover, the ZnO film deposited at high temperature (400 °C) shows a reduced carbon content respect with the low temperature sample (300 °C), as expected from a smoother surface as well as from the higher deposition temperature. As to the ZnO sample deposited at 250 °C,

the detected amount of Zn is very small (about 2%). Therefore we can set the MOCVD deposition threshold above the temperature of 250 °C.

By applying the above discussed deposition conditions to deposit ZnO on silicon substrates patterned by colloidal lithography, the formations of ZnO nanohole arrays are successfully achieved, as shown in Fig. 3, where the ZnO nanospheres are obtained both at 300 °C, 40 min (Fig. 3a) and 400 °C, 5 min (Fig. 3b).

Finally, the effect of Ag catalyst concentrations on deposited ZnO morphology is discussed. Ag(hfa)tetraglyme [19] ethanolic solutions (0.1 M and 0.01 M) have been deposited either by drop casting or spin
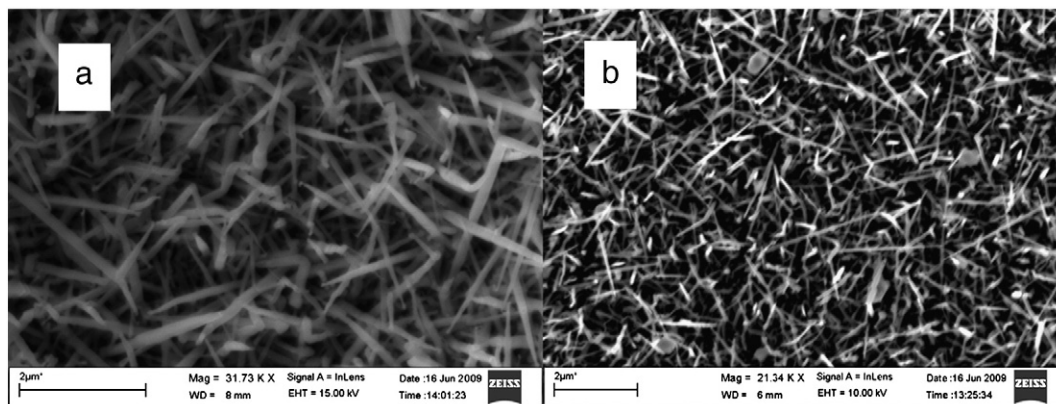
Fig. 5. SEM images (scale bar= 2 micron) of ZnO nanowires growth (on silver catalyst) at 600 °C after 1 hour deposition (a) and 30 min deposition (b).
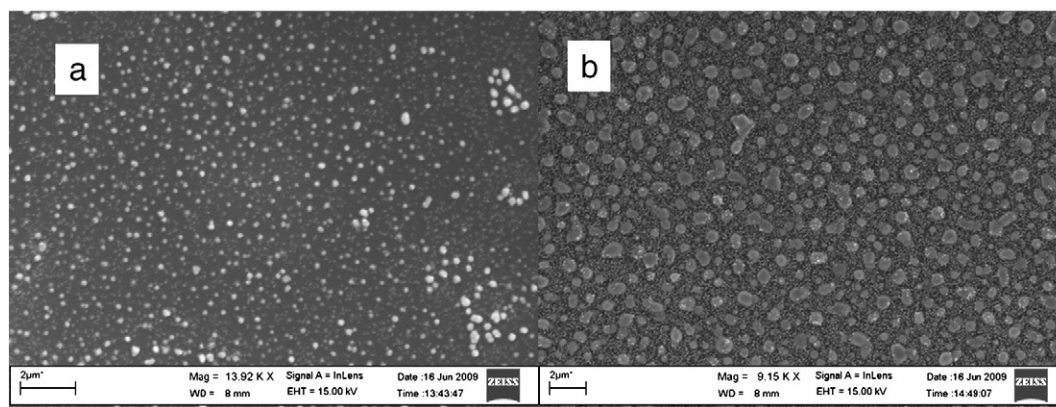
Fig. 6. SEM images (scale bar = 2 micron) of ZnO film deposited at 400 °C, 30 minutes on Ag catalyst layer at the initial concentrations of 0.01 M (a) and 0.1 M (b).
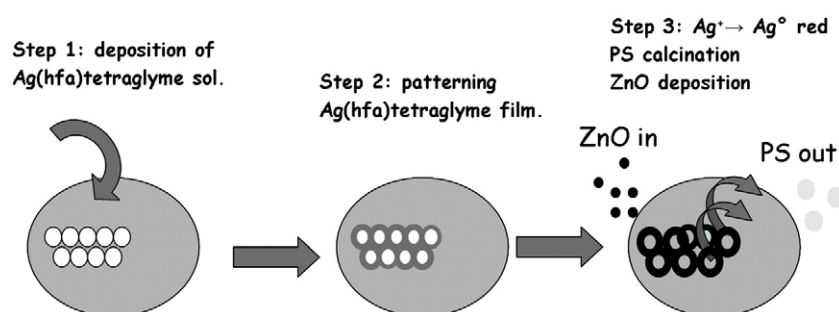

Fig. 7. A schematic representation of the process sequence adopted to fabricate ZnO ordered nanoholes array.

coating on silicon substrates. A further annealing in air, performed at 400 °C for 30 min, is used to reduce Ag$^+$ ions to metallic silver. The obtained nanostructured films are composed of discrete silver grains, whose dimensions depend on the deposition technique, spin coating vs drop casting (Fig. 4). In fact, the spin coated layers present an average dimensions of about 100 nm (Fig. 4a), that increase up to 300 nm, for the drop casted ones (Fig. 4b), due to grain coalescence effects.

ZnO has been deposited by MOCVD on the substrates pre-coated with the silver catalyst films. Different process conditions have been used to study how the catalytic effect can tailor the ZnO film morphology. A massive ZnO nanowire production is promoted by high deposition temperature (600 °C, 1 h, Fig. 5a) [18], using a 0.01 M Ag catalyst initial concentration, despite short process deposition times (600 °C, 30 min, Fig. 5b). Only at low deposition temperatures, not higher than 400 °C, the ZnO film morphology changes significantly, thus replicating the original catalyst nanostructure. Using these low temperature conditions the overall film morphology appears sensitive to both catalyst initial concentration and ZnO deposition time (Fig. 6). In fact, after 30 min of ZnO deposition on silver catalyst (initial precursor concentration of 0.01 M) the pristine Ag grains distribution is still visible and no significant ZnO growth is observed between the grains (Fig. 6a).

On the other hand, a more extensive growth is observed when deposition time is increased up to 60 min and/or when a higher catalyst precursor concentration (0.1 M) is used (Fig. 6b).

These findings indicate a strong catalytic effect of the silver metal-organic precursor on ZnO growth and suggest that a proper tuning of the deposition process parameters (i.e., low catalyst concentrations, deposition temperature below 400 °C, short process time) limits and controls the high yield production of ZnO nanowires. Moreover, the accurate matching of both catalyst precursor concentrations and ZnO deposition process conditions is required for an effective integration of

catalyst assisted MOCVD process with colloidal lithography (Fig. 7) driving the formation of ordered ZnO nanoholes array [18].

4. Conclusions

The presented results demonstrate an easy route to control the morphology of ZnO films deposited by MOCVD. Indeed the formation of ZnO nanowires can be finely tuned through the accurate control of the initial concentration of Ag catalyst precursor as well as of the ZnO growth process parameters, such as temperature and deposition time. This process tuning is also required for an effective integration of the MOCVD deposition process with colloidal lithography to obtain ordered ZnO nanoholes array [18]. The possibility to simply modify both the concentration of metal-organic precursor solutions, easily deposited (spin coating or drop casting) on any kind of substrate and the ZnO MOCVD process conditions, makes the proposed hybrid approach valuable to fabricate nanoporous ZnO based layers with remarkable high surface areas. Such nanostructures are promising for a wide variety of applications including bioengineering, catalysis, environmental engineering and sensor systems.

References

[1] X. Wang, J. Song, Z.L. Wang, J. Mater. Chem. 17 (2007) 711.
[2] Z.L. Wang, ACS Nano 2 (10) (2008) 1987.

[3] X. Duan, Y. Huang, Y. Cui, J. Wang, C.M. Lieber, Nature 409 (2001) 66.
[4] Y. Huang, X. Duan, Y. Cui, L. Lauhon, K. Kim, C.M. Lieber, Science 294 (2001) 1313.
[5] J.H. Song, X.D. Wang, E. Riedo, Z.L. Wang, Nano Lett. 5 (2005) 1954.
[6] F. Patolsky, C.M. Lieber, Mater. Today 8 (2005) 20.
[7] Z. Zhang, S.J. Wang, T. Yu, T. Wu, J. Phys. Chem. C 111 (2007) 17500.
[8] M. Kirkham, X. Wang, Z.L. Wang, R.L. Snyder, Nanotechnology 18 (2007) 365304.
[9] X. Wang, J. Song, C.J. Summers, J.H. Ryou, P. Li, R.D. Dupuis, Z.L. Wang, J. Phys. Chem. B 110 (2006) 7720.
[10] C. Li, G. Fang, Y. Ren, Q. Fu, X. Zhao, J. Nanosci. Nanotechnol. 6 (2006) 1467.
[11] J. Rybczynski, D. Banerjee, A. Kosiorek, M. Giersig, Z.F. Ren, Nano Lett. 4 (10) (2004) 2037.
[12] M.H. Huang, Y. Wu, H. Feick, N. Tran, E. Weber, P. Yang, Adv. Mater. 13 (2) (2001) 113.
[13] X. Wang, C.J. Summers, Z.L. Wang, Nano Lett. 4 (2004) 423.
[14] J.H. Moon, W.S. Kim, J.-W. Ha, S.G. Jang, S.-M. Yang, J.-K. Park, Chem. Commun. 32 (2005) 4107.
[15] L.S. McCarty, A. Winkleman, G.M. Whitesides, Angew. Chem. Int. Ed. 46 (2007) 206.
[16] S.-M. Yang, S.G. Jang, D.-G. Choi, S. Kim, H.K. Yu, Small 2 (4) (2006) 458.
[17] J.-H. Lee, I.-C. Leu, Y.-W. Chung, M.-H. Hon, Nanotechnology 17 (2006) 4445.
[18] M.E. Fragalà, C. Satriano, G. Malandrino, Chem. Commun. 7 (2009) 839.
[19] M.E. Fragalà, G. Malandrino, O. Puglisi, C. Benelli, Chem. Mater. 12 (2000) 290.
[20] M.E. Fragalà, G. Compagnini, G. Malandrino, C. Spinella, O. Puglisi, Eur. Phys. J. D 9 (1999) 631.
[21] G.M.L. Messina, C. Satriano, G. Marletta, Chem. Commun. 40 (2008) 5031.
[22] G. Malandrino, M. Blandino, L.M.S. Perdicaro, I.L. Fragalà, P. Rossi, P. Dapporto, Inorg. Chem. 44 (2005) 9684.